Supporting Information

Peresani et al. 10.1073/pnas.1016212108

SI Text

Presentation of Fumane Cave. The opening of the Fumane Cave lies at the base of a rock cliff at 350 m above sea level (ASL) on the left slope of the valley of a small tributary stream flowing eastward to join the main Fumane valley in the Monti Lessini in the Veneto Prealps. This important site was already known in the 19th century, and the first explorations were carried out by the Natural History Museum of Verona in 1964 and 1982 at the bottom of a sequence exposed by a road cutting in 1950. A new series of investigations started in 1988 under the patronage of the Superintendence for the Archeological Heritage of Veneto, bringing to light a sequence of Paleolithic occupations. Excavations are conducted on a regular basis every year by the universities of Ferrara and Milan I.

The cave is part of a fossil karst complex excavated in the Ooliti di San Vigilio carbonatic sandstone (upper Lias), extensively dolomitized in the valley where the cave opens. The cave conjoins with other tunnels and was completely obstructed by sediments and by the collapse of the external vault. After this landslide was removed, between 1990 and 1996, a sheltered area of almost 60 m^2 was brought to light and extensive excavations began, with the aim of investigating evidence of the final Mousterian and Aurignacian occupations.

Sedimentary Sequence. The whole complex preserves sedimentary sequence 12 m thick, divided into four macrounits labeled S, BR, A, and D, which record the main climatic events occurring from the Early Weichselian to the second half of the Middle Weichselian. These four macrounits have been defined on the basis of their lithological composition or degree of anthropization. The base is a fill originating with the deposition of residual dolomitic sands covered by a megabreccia with partially weathered boulders. It represents the opening event preceding the Pleistocene long-term aggradation recorded, starting from macrounit S. In this first sedimentary body, dolomitic sands are prevalent, mixed with local limestone slabs in beds alternating with human occupations. Above this, the macrounit BR marks a clear lithological change due to the dramatic decrease in sands and the increase in aeolian loam with frost-shattered slabs. With the exception of the paleo living floor BR11, Mousterian occupations are evidenced only by a few dispersed lithic tools, faunal remains, and, in some cases, hearths with associated artifacts and bones interpreted as relics of specific tasks accomplished during short-term occupations. Due to intense anthropization, the overlaying macrounit A includes several horizontally layered beds from A13 to A1. Mousterian living floors range from units A11 to A5, Uluzzian from A4 to A3, and Aurignacian from A2 to A1.

The horizontally stratified final Mousterian units include frost-shattered breccia, colluvial sands (A13–A12), and aeolian matrix (A11–A4) that gradually prevail over stones to become exclusive outside the present-day cavity. The variable content in these basic lithological components and the degree of anthropization are the distinctive elements of the overall stratigraphic sequence. Furthermore, each unit contains different *facies* related to the granulometric variability, marking distinct sedimentary contexts in the cave. In detail, units A13 and A12 are loose breccia with high sand content; stones are mostly vertically arranged and outline narrow deformations that affect the overlaying unit (A11) incorporating portions of anthropic sediment. A11 and A10 are strongly anthropized levels interstratified with stony and sterile levels of frost slabs. Units A9 and A8 are still frost-shattered loose breccia with scarce-to-prevalent aeolian matrix, covered by unit A7, a sterile level with clayey-loamy matrix and smoothed coarser elements that marks a clear, unilinear boundary with the overlaying unit (A6). This is a thin-plane anthropic horizon included in the complex described in the specific section below. The uppermost unit A4 is a breccia with slabs (A4I–A4III), which are prevalent at the cave entrance and transitional to a loamy layer outside the cavity (A4IV).

Macrounit D tops the sequence occluding the cavities and outlining the present-day slope morphology. Its origin is mainly due to several landslide events followed by stabilization and affected by crioturbation during the interval from part of OIS3 to OIS2. Human presence, still marked in the lower Aurignacian units (D3d, D3b, and D3a), becomes sporadic in the middle level D1d, where some Gravettian artifacts have been found.

Paleocology. Macromammals, in particular hunted ungulates, indicate moist-cool climatic phases when forests extended over alpine grasslands. Nevertheless, ibex, chamois, and marmot, in addition to some birds—Alpine chough and *Lagopus muta*—indicate that open alpine environments still existed near the cave. Cervids prevail over caprids in macrounit S, although episodes of climatic cooling have been identified in S9 and in S3, where the ratio reverses. In macrounit BR a first phase records the prevalence of cervids again, with a more marked presence of caprids in BR6 up to a maximum in BR1. Cervids still prevail in A13–A12, A11–A10, and A6–A5 until the abrupt replacement by ibex and chamois in coincidence with the first Aurignacian in A2 and the spread of alpine grassland.

Anthracological investigations record a high *Pinus sylvestris*/*mugo* content in A11–A10 and a decrease in A9 until its disappearance from A7 upward. The percentage of *Larix decidua* remains high, and only in unit A11 does it become subordinate to *Pinus*. The anthracological association from unit A7 to A4 also includes a few broadleaf remains. Arboreal vegetation constituted a sort of parkland, variably closed during the late Mousterian. Not surprisingly, these formations were probably a sort of transition to the glacial-type herbaceous vegetation.

Final Mousterian A5–A6 Stratigraphic Complex: General Information. ***Excavation and stratigraphy.*** The final Mousterian and Uluzzian layers have been excavated at different times since 1989 and to different extents in the area behind the present-day cave drip line and in the cave entrance (Fig. S2). The first complete stratigraphy was exposed in 1989 and 1990 in the southernmost sector; from there a northwest-to-southeast trench was opened in 1990 toward a central zone just in front of the cave entrance. Units A9 to A4 were further exposed in 1995 and 1996 in two narrow trenches dug inside the cave, before the A5–A6 complex was extensively excavated in 2000, 2001, and 2006–2008. These excavations involved several units (TettoA5, A5, A5BR, A5+A6, A6, A6BR) and brought to light combustion structures, scattered ungulate bones, flint, and other stone artifacts. All units have been excavated in 33 × 33-cm squares, with dry collection of materials (bones and lithics) and then by wet sieving. All flints ≥3 cm, macrotools on pebble, manuports, and large charcoal, as well as bones and teeth that were either identifiable or ≥5 cm have been mapped on site.

The sedimentary units of the A5–A6 complex lay over A7, a layer completely lacking in primary cultural traces, and form a homogeneous subhorizontal body with a slight east/southeast and northeast slope, just a little less than 20 cm thick. The uppermost units A4 and A3 are stony or sandy layers with few cultural remains progressively replaced by aeolian dust in the

outermost part of the cave. From the inner to the outermost zone of the cavity, aeolian dust gradually substitutes stones to become exclusive. The main units are as follows:

A6 is a layer with a dense quantity of organic matter, charcoal, fauna, and lithic artifacts as well as several combustion structures. It is 3–8 cm thick and gradually becomes thinner toward the wall, decreasing to a fine sheet of about 1–2 cm; in the inner part of the cavity it shows major variations in the form of folds, due to cryogenic/pressure structures.

A5+A6 is a loose breccia, richer in stones in the cave entrance than beyond the present-day drip-line belt. It is about 10 cm thick and systematically covers A6.

A5 is a horizon with combustion structures and dump material brought to light in the westernmost zone and gradually vanishing in the rest of the excavated area.

Field archaeological evidence. A6 is divided into three zones: the western zone, protected by the two main galleries, where there are over 20 combustion structures and localized accumulations of burnt products; a discard area characterized by the accumulation of materials derived mainly from combustion or altered by heating; and finally a large area extending to the opposite wall with dense scatters of lithic artifacts, tools, and bones modified by humans.

Combustion structures are rarely larger than 30 cm and are characterized by a reddened horizon often covered by a charcoal layer, microcharcoal, ash, and dispersed organic matter. Such structures are set directly over the sands of the sterile unit A7, but may also be within or at the top of A6. Therefore, these structures mark the aggradation of this unit and document a sequence of human frequentations that maintain the general spatial organization of the activities over time. Human occupations are more ephemeral and less intense in the above complex, where unit A5 +A6 supports the discontinuous layer A5 with its combustion structures and charcoal concentrations. Level A5 preserves a combustion area (structure A5-SIII) associated with artifacts in the immediate vicinity and partially surrounded by squared slabs.

Radiocarbon dates. >Levels A5 and A5+A6 have been recently radiocarbon dated by Oxford Radiocarbon Accelerator Unit (ORAU) using ABOX-Sc treatment. Dates are consistent for layer A5 (OxA-17980: 40150 ± 350 B.P.), structure A5-SIII (OxA-X-2275-45: 41650 ± 650), level A5+A6 (OxA-17566: 40460 ± 360 B.P.). Using a modeled Bayesian sequence generated with OxCal 4.0, Higham et al. (1) suggest that the latest Mousterian occupation of A5 took place before 43,580–42,980 BPCARIACO-HULU at 68.2% confidence.

Lithic assemblage. Thousands of artifacts have been produced using the Levallois technique; the aim was to obtain extremely functional Levallois blades with symmetrical or convergent edges using the unidirectional recurrent modality almost until the terminal phase of the reduction sequence, when it was replaced by the centripetal modality until the final discarding of the core. This type of Levallois reduction sequence was previously used in units A11, A10V, and A10, on locally provisioned flints. Levallois predetermination was not the exclusive method. A different scheme focuses on the manufacture of small flakes from polyhedral cores. A second scheme is comparable to discoid production, comparable to the discoid industry of unit A9. A third scheme involves the manufacture of a very small number of bladelets from cores and flake cores, prepared briefly with a single striking platform.

Retouched tools are mainly scrapers in contrast to points, notches, and denticulates, with the latter being rare, together with thinned simple flakes and other specimens. Of the scrapers, the simple types predominate over double, convergent, and transversal ones, as well as over scrapers with alternate or marginal retouch. Furthermore, the frequency of points and convergent scrapers in units A5 and A5+A6 and, occasionally, in unit A6, should be noted. These are artifacts made on Levallois blades and elongated and partially cortical flakes, selected not only for their morphological and geometric regularity, but also because of their thickness. Retouchers are associated with retouched tools: more than half of the 75 recorded ones were found in layer A6. Except for an antler object from A6, only long bone and metapodial diphyseal fragments belonging to cervids and less frequently to caprids have been used. Finally, there is the exceptional presence of a scraper made on the diaphysis of a large ungulate.

Taphonomic Analysis of Bird Remains. Some of the traces detected in this study could not be referred with certainty to the action of a lithic tool. These striae, however, show some of the micromorphological features typical of cut marks, and the location on the anatomical element is also indicative of a butchering action. Also, traces such as these have been identified only on wing bones.

Of the sample analyzed, consisting of 404 elements (Table S1), wing bones (humerus, radius, ulna, carpometacarpus, and wing carpals and phalanges) constitute about 43% (Nisp 173). Of these 173 elements, 12 (about 7%) bear traces that are anthropic, or interpretable as such. These traces are present on six (22%) of the 22 species in the sample. The total number of wing elements of these six species is 141, ∼9% of which bear modifications relating to wing utilizations.

Oblique traces, deep and repeated, have been identified on the lateral face of the distal epiphysis of a right ulna of *Pyrrocorax graculus*. These are wide, positioned longitudinally to the main axis of the bone and show partial recent flaking of the surface (Fig. S2 *A* and *B*). In addition, there is a single deeper groove with a V-shaped cross-section and two parallel traces preserved at its bottom. Traces such as these cannot be attributed with certainty to the repeated action of a lithic tool. On the opposite face, at the end of the articulation, some surface removals can be recognized, which may be related to peeling (Fig. S2 *C* and *D*).

A distal carpometacarpus of *Lagopus* cf. *lagopus* shows two transversally oriented striae on the diaphysis, together with a third oblique one (Fig. S3). Only the central one has a bottom and edge morphology similar to that produced by a lithic tool (Fig. S3*B*).

A right distal humerus of *Pyrrocorax graculus* shows fracture edges that may suggest fresh bone fracturing (Fig. S3*C*). On the caudal face there is a crushing (*enfoncement*) produced by the olecranon of the ulna on the sulcus musculi humerotriceps of the humerus (Fig. S3*D*). This modification is produced by forcedly flexing the two elements in the opposite direction to the natural articulation. On the caudal face of the distal epiphysis on the processus flexorius, peeling traces have also been detected at the insertion point of the triceps humeralis (Fig. S3*E*).

Other traces of peeling, as well as those on the ulna of Alpine chough with the cut marks described in the article (Fig. 3*A*) and those illustrated above (Figs. S2 *C* and *D* and S3*E*), have been identified on another humerus of *Pyrrocorax graculus*, localized at the same point (Fig. S4*B*), and on a fragment of tarsometatarsus of an indeterminate Aves.

Arrachement traces have been identified on a proximal ulna of *Tetrao tetrix* associated with a fresh bone fracture along the diaphysis (Fig. S5 *A–C*). The *arrachement* is a fracture of the olecranon on the proximal articulation of the ulna produced during disarticulation by forced stretching of the elbow joint.

Fractures produced by torsion as well as fresh bone fractures have been identified on several specimens belonging to different species (Fig. S5 *D* and *F*); in rare cases even small notches have been recognized (Figs. S4*C* and S5*D*). It is important to note that the fresh bone fracture edges are always present on specimens showing other traces (cut marks, peeling, *enfoncement*, *arrachement*) presumably produced by humans. Of particular interest, on the distal portion of a left carpometacarpus of Eurasian black vulture (*Aegypius monachus*; Fig. 4) is the cooccurrence of clear

disarticulation cut marks and polishing associated with microstriae on the fracture edge (Fig. S6). There are also frequent specimens belonging to different species (in particular, *Pyrrocorax graculus* and *Crex crex*) that show scoring and crushing produced by the pressure of carnivore teeth (Fig. S7 *A* and *B*). Some of these gnaw marks could possibly be traces of human teeth, but at the time it was not possible to verify this hypothesis. Rare rodent gnaw marks are also present. There are also bones with corrosion traces, probably produced by gastric digestive juices of carnivores and/or raptors (Fig. S7*C*).

On many specimens there are also striae of uncertain origin, isolated or in groups, superficial, very short, with variable orientation, sometimes with erosion traces that prevented the certain identification of the producing agent, although most of these striae could be the result of trampling (Fig. S4 *D* and *E*).

1. Higham T, et al. (2009) Problems with radiocarbon dating the Middle and Upper Palaeolithic transition in Italy. *Quat Sci Rev* 28:1257–1267.

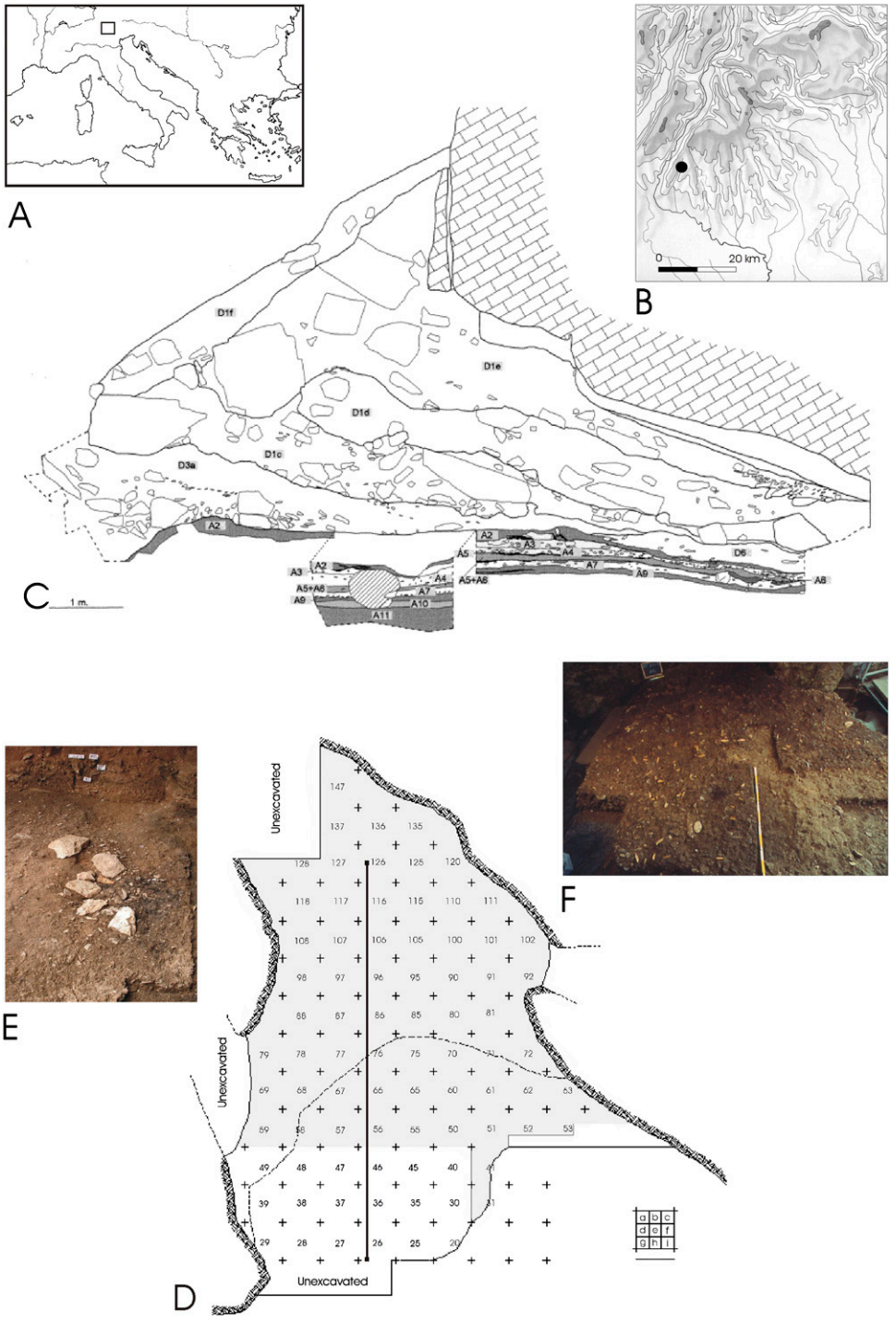

Fig. S1. (*A*) Position in the north of Italy on the Monti Lessini Plateau and (*B*) the Fumane Cave. (*C*) Sketch sagittal section of the cave with evidence of the late Mousterian (A11–A5), Uluzzian (A4–A3), and earliest Aurignacian layers (A2) and of their variable content in archaeological remains (increasing from light gray to dark gray and black; by M. Cremaschi & M. Peresani, redrawn by S. Muratori; ref. 1). (*D*) Plan of the cave entrance and the lateral tunnels showing the grid and the subgrid (*Lower Right*); light gray, the excavation of the stratigraphic complex A5–A6. Solid line from squares 26–126 outlines the sagittal section. The present-day drip line is projected to the ground by the dotted line. (*E*) Large fireplace found in layer A5, squares 77–78/87–88. (*F*) Layer A6 in course of excavation in the eastern half at the cave entrance.

1. Peresani M, et al. (2008) Age of the final Middle Palaeolithic and Uluzzian levels at Fumane Cave, Northern Italy, using ^{14}C, ESR, $^{234}U/^{230}Th$ and thermoluminescence methods. *J Archaeol Sci* 35:2986–2996.

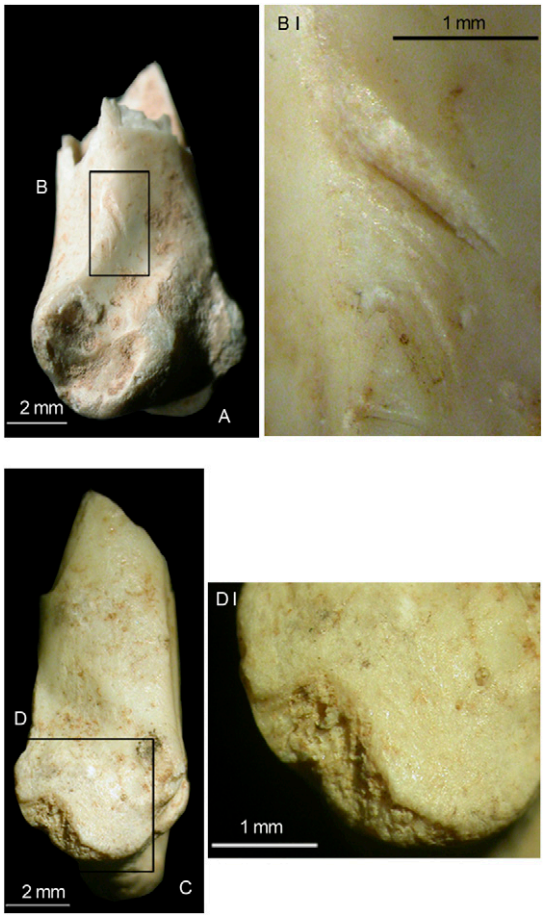

Fig. S2. Right distal ulna of Alpine chough (*Pyrrocorax graculus*). (*A*) Medioventral view. (*B*) Localization of the probable cut marks; (*B*, I) close-up. (*C*) Dorsal view. (*D*) Localization of the peeling traces; (*D*, I) close-up.

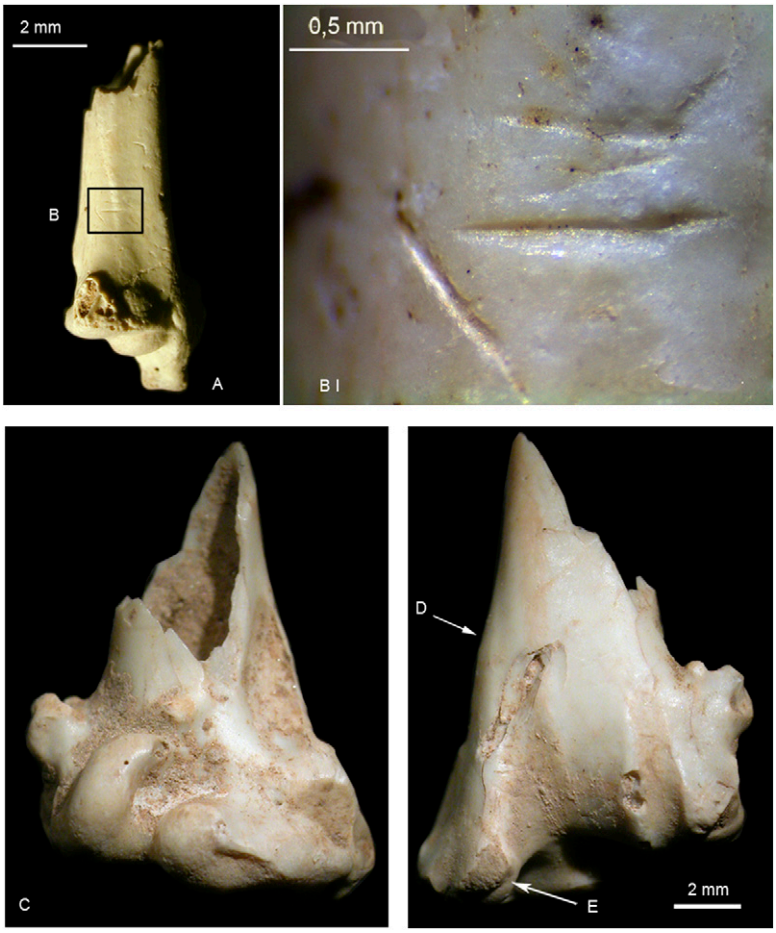

Fig. S3. (*A*) Lateral view of the right distal carpometacarpus of willow ptarmigan (*Lagopus* cf. *lagopus*). (*B*) Localization of the probable cut marks; (*B*, I) close-up. (*C*) Fracture on the cranial side of the right distal humerus of Alpine chough (*Pyrrocorax graculus*). (*D*) Localization of the *enfoncement* on the caudal side. (*E*) Localization of the peeling traces.

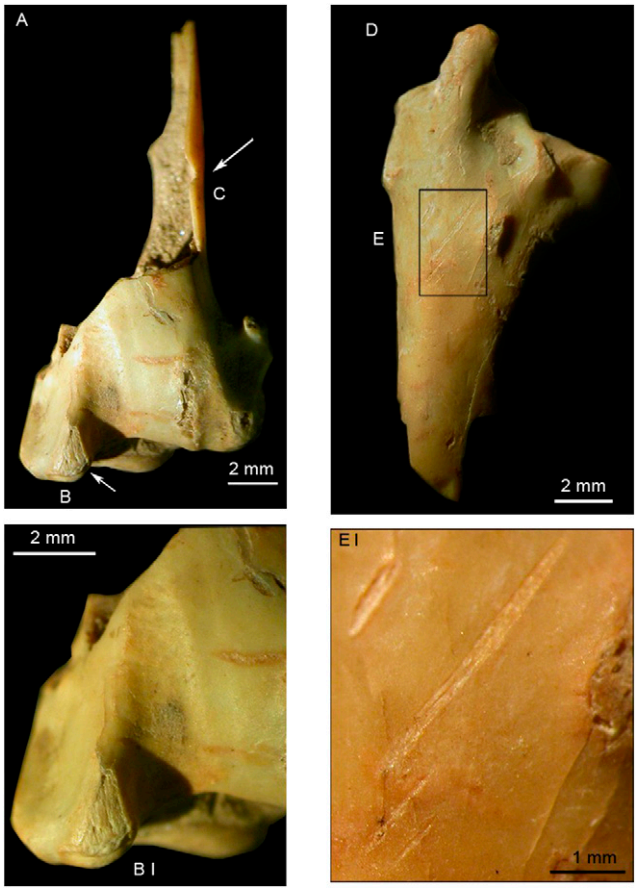

Fig. S4. (*A*) Right distal humerus of Alpine chough (*Pyrrocorax graculus*). (B) Localization of the probable peeling traces on the caudal side; (*B*, I) close-up. (*C*) Localization of a small notch. (*D*) Medioventral view of a right proximal ulna of Alpine chough (*Pyrrocorax graculus*). (*E*) Localization of striae of uncertain origin, probably due to trampling; (*E*, I) close-up.

Fig. S5. Right proximal ulna of black grouse (*Tetrao tetrix*). (*A*) Ventral view. (*B*) Medioventral view. (*C*) Localization of the *arrachement*; (*C*, I) close-up. (*D*) Localization of a small notch and (*E* and *F*) fresh bone torsion fractures on three diaphyses of indeterminate bird.

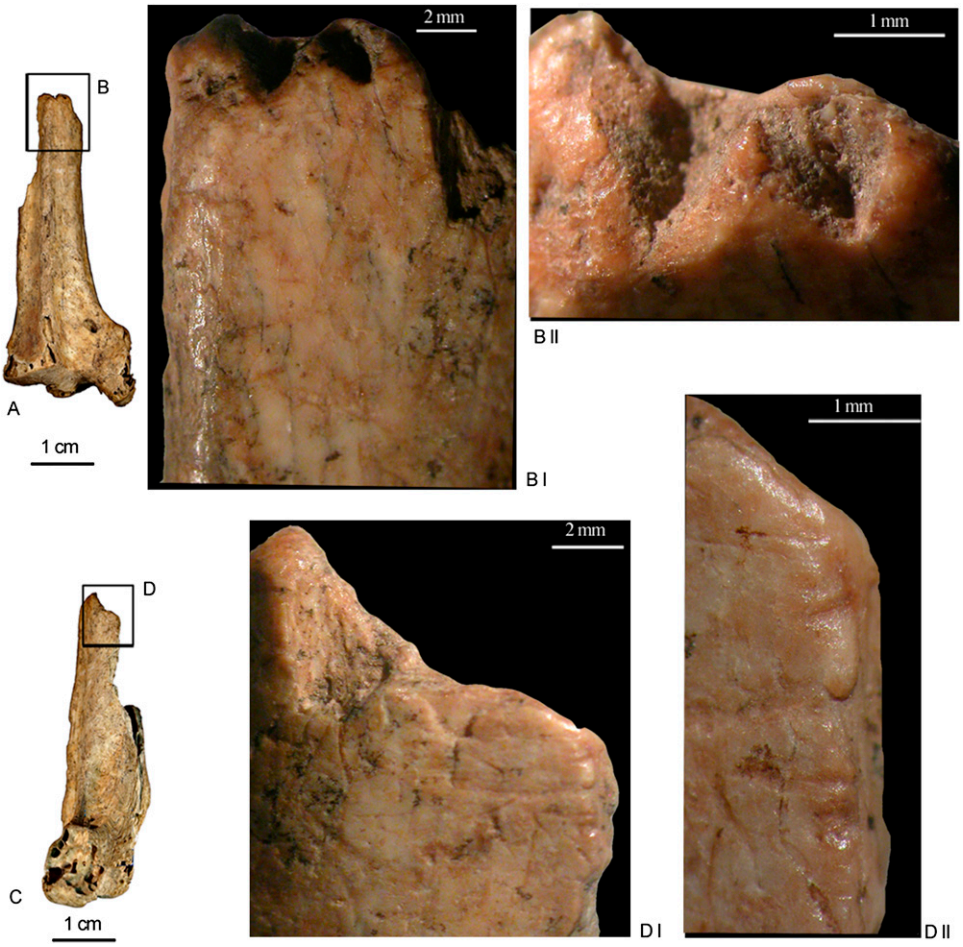

Fig. S6. Wear traces on a left carpometacarpus of Eurasian black vulture (*Aegypius monachus*). (*A*) Dorsal view. (*B*) Localization of the traces; (*B*, I and II) close-ups. (*C*) Medioventral view. (*D*) Localization of the traces; (*D*, I and II) close-ups (see also Fig. 4).

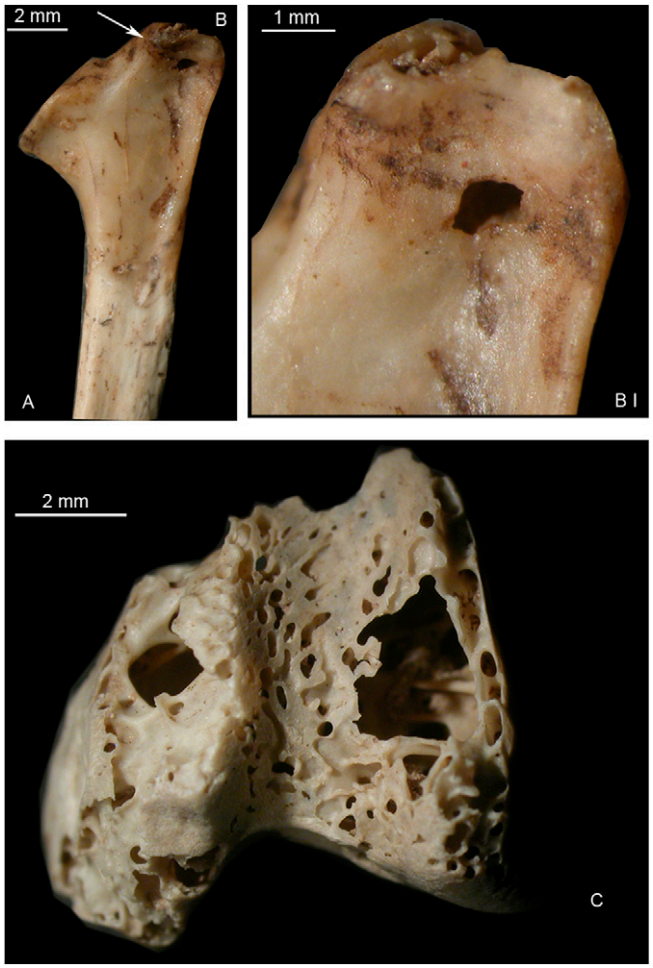

Fig. S7. (*A*) Ventral view of a right scapula of corn crake (*Crex crex*). (*B*) Localization of scoring and puncture traces; (*B*, I) close-up. (*C*) Cranial view of a right distal femur of black grouse (*Tetrao tetrix*) with corrosion traces produced by gastric digestive juices.

Table S1. Birds from the Mousterian levels and from levels A5–A6 of Fumane Cave

Species	Total NISP A6–A5	%	Total MNI A6–A5	%
Lammergeier (*Gypaetus barbatus*)	1	0.3	1	2.0
Eurasian black vulture (*Aegypius monachus*)	1	0.3	1	2.0
Common kestrel (*Falco tinnunculus*)	11	3.7	3	6.0
Red-footed falcon (*Falco vespertinus*)	5	1.7	2	4.0
Eurasian hobby (*Falco subbuteo*)	4	1.4	3	6.0
Willow ptarmigan (*Lagopus* cf. *lagopus*)	1	0.3	1	2.0
Rock ptarmigan (*Lagopus muta*)	2	0.7	1	2.0
Black grouse (*Tetrao tetrix*)	30	10.2	5	10.0
cf. Black grouse (*Tetrao tetrix*)	9	3.1		
Common quail (*Coturnix coturnix*)	2	0.7	1	2.0
Galliformes indet.	3	1.0		
Water rail (*Rallus aquaticus*)	1	0.3	1	2.0
Corn crake (*Crex crex*)	40	13.6	9	18.0
cf. Corn crake (*Crex crex*)	7	2.4		
cf. Common moorhen (*Gallinula chloropus*)	1	0.3	1	2.0
Rallidae indet.	3	1.0		
cf. Northern lapwing (*Vanellus vanellus*)	1	0.3	1	2.0
Eurasian woodcock (*Scolopax rusticola*)	3	1.0	1	2.0
Common wood pigeon (*Columba palumbus*)	1	0.3	1	2.0
Long-eared owl (*Asio otus*)	4	1.4	4	8.0
Asio sp.	2	0.7		
Tengmalm's owl (*Aegolius funereus*)	2	0.7	1	2.0
Eurasian golden oriole (*Oriolus oriolus*)	1	0.3	1	2.0
Common magpie (*Pica pica*)	3	1.0	1	2.0
Alpine chough (*Pyrrhocorax graculus*)	103	35.0	9	18.0
cf. Alpine chough (*Pyrrhocorax graculus*)	27	9.2		
Common raven (*Corvus corax*)	1	0.3	1	2.0
Corvidae indet.	7	2.4		
Common crossbill (*Loxia curvirostra*)	1	0.3	1	2.0
Passeriformes indet.	17	5.8		
Total identified birds	294	100	50	100
Identified birds	294	45		
Unidentified birds	110	16.7		
Aves being identified	256	38.8		
Total bird remains	660	100		

NISP, no. of identified specimens; MNI, minimum no. of individuals.